Ultrafast Intermolecular Electron Transfer Dynamics: Perylene in Electron-Accepting Micellar Medium

Ajay K. Singh, Jahur A. Mondal, G. Ramakrishna, Hirendra N. Ghosh, Tusar Bandyopadhyay, and Dipak K. Palit*

Radiation Chemistry & Chemical Dynamics Division, Bhabha Atomic Research Centre, Mumbai-400085, India

Received: October 5, 2004; In Final Form: December 10, 2004

The dynamics of ultrafast photoinduced intermolecular electron transfer (ET) from the excited singlet (S_1) state of perylene (Pe) to an electron-accepting cationic surfactant molecule, *N*-cetylpyridinium chloride (CPC), in aqueous micellar solutions has been investigated using the femtosecond transient absorption spectroscopic technique with temporal resolution of 120 fs. The Pe molecule is localized at or near the micellar surface, where it coexists with the pyridinium moieties (headgroups of the micelle) of the surfactant molecule. Following photoexcitation of Pe, an electron is transferred to the neat and geometrically restricted headgroup of the micelle. Dynamics of the forward ET process as well as the geminate recombination or back ET (BET) process have been followed by monitoring the temporal evolution of the S_1 state of Pe and the cation radical of Pe ($Pe^{\cdot+}$), respectively. The multiexponential forward ET process indicates that the ET dynamics is highly correlated with the spatial distributions of the micellar headgroups around a donor Pe molecule and thus dependent on the donor−acceptor distance. The distance-dependent ET and BET rates have been calculated following the method of Weidemaier and Fayer (*J. Chem. Phys.* **1995**, *102*, 3820) to get the best fit parameters for the multiexponetial temporal profiles for the S_1 state of Pe as well as $Pe^{\cdot+}$. Because the acceptor is a constituent of the neat micellar medium, their confinement on the surface of the microheterogeneous medium provides a very large concentration such that, even though the forward transfer rate is 0.06 ps^{-1} at the distance of closest approach, the ET process is complete within a 200-ps time domain. If the concepts of distribution of ET distances are utilized, the possible role of material diffusion on the kinetics of forward ET is ruled out. This is an experimental study to show, for the first time, the ultrafast distance-dependent light-induced ET dynamics following both the excited state of the donor and the cation radical formed in an ET process using the transient absorption spectroscopic technique in a self-reactive restrictive environment.

1. Introduction

Photoinduced electron transfer (PET) reactions have attracted a great level of attention from physical chemists because of their relevance in many physical, chemical, biological, and technical processes.[1−6] A basic understanding of the mechanism of the electron transfer (ET) process has both fundamental and practical implications ranging from photosynthesis,[7] biological redox processes,[2] and design of the devices for solar energy conversion and storage[8,9] to photonics and molecular electronics.[10−12] Numerous studies have been performed to understand the influence of different kinds of environments including homogeneous liquids[13−16] as well as heterogeneous media, such as micelles,[17−22] vesicles,[23] proteins,[24] and DNA.[25,26] Dependence of ET processes on the structural geometry and the spatial and distance distribution of the donors and acceptors, as well as characteristics of local environments, have also been studied by numerous groups.[17,23,26−28] One of the goals in the area of ET research is to thematically understand the construction and optimization of the perfect structural geometry and the precise spatial arrangement of the donor and acceptor moieties in photosynthetic reaction centers, which minimizes the backward electron transfer (BET) rate to provide unit efficiency for the forward ET process.[7]

Most of the work on ET systems can be broadly classified into two groups. The first group includes the intramolecular ET systems, where the donor and acceptor moieties are part of a bichromophoric molecule linked to each other through a spacer group.[12,29,30] Valuable information regarding free energy, distance, and spatial dependence of ET reactions has been obtained by varying the characteristics of the donor and acceptor groups as well as the length and nature of the spacer groups. The second group deals with intermolecular ET systems, where a number of quencher molecules may exist in a complicated spatial distribution with respect to the donor molecule. ET reactions in restricted geometrical systems, such as micelles and vesicles, have received a great deal of interest because of their potential to have a better yield of the forward ET reaction due to the reduced rate of the BET process.[23,31,32] This is an important goal of ET studies aiming to develop efficient energy conversion and storage devices. Because of the multiphase character and constrained geometries, micelles and vesicles have been proven to be useful media in isolating the counter radical ions produced because of ET reactions by slowing down the rate of geminate recombination and increasing the overall yield of the forward process. On the other hand, because the ET process, which occurs within a short range of molecular distances (e.g., a few angstroms), is sensitive to the nature of the local environment, this process may also be a useful probe for characterization of the micelle environment.[33]

* Author for correspondence. E-mail: dkpalit@apsara.barc.ernet.in. Phone: 91-22-25595091. Fax: 91-22-25505151/25519613.

10.1021/jp045481d CCC: $30.25
Published on Web 02/05/2005

PET processes in micelles and vesicles are complex because of microheterogeneity of the media. The ET process is expected to be strongly influenced by the restricted, nonisotropic spatial structure of the micelle**.** The micellar medium is characterized as having a nonpolar core region and headgroup region (or Stern layer) surrounded by bulk water medium.[33] The polarity of the headgroup region depends on the kind of micelle, whether positive, neutral, or negative. Because of the differences in the properties of the headgroup and core regions of micelles, different types of water-insoluble molecules are expected to locate selectively in the two regions. However, there is considerable debate about the exact location of the probe in the micelle. In many cases, a spatial distribution of probe molecules in these two regions is more likely.[34] In such a case, no definite value of the rate constant for the ET process can be assigned because of varying polarities of the heterogeneous reaction zones as well as the distance dependence of the ET rate due to spatial distributions of the reactants. It has been found both experimentally and theoretically that, in many systems, the transfer rate can be modeled as having an exponentially decaying distance dependence on a distance scale of a few angstroms.[34,35] The most straightforward spatial distribution is where a donor is surrounded by acceptors, which are randomly distributed in an infinite three-dimensional homogeneous and isotropic medium. However, the spatial distribution of the acceptors with respect to the donor can have a profound effect on ET dynamics in heterogeneous media like micelles and vesicles. These are the systems which are not infinite in extent and do not involve the whole ensemble of molecules dissolved in the reaction bath, as well as concentrations of the reactants are not well-defined. It is evident that, in such a case, the rate laws derived for a homogeneous system are no longer valid, because theoretical analysis of any observation depends on the way the ensemble averages are performed.[17−20] In particular, in the case of a heterogeneous system, the fact has to be taken into account that compartmentalization of the reactants changes their spatial ordering as a consequence of their association with the surfactant aggregates as compared to the three-dimensional homogeneous system. While exchange of the reactants between the different regions of the micelle is more sluggish than the reaction time, the reaction essentially takes place within the isolated confined region of the host aggregate where the effective local reactant concentration can be considerably higher.

The forward transfer problem for PET in isotropic three-dimensional systems, in which the reactants are fixed-point particles and randomly distributed, has been solved exactly when the distance dependence of the ET rate is modeled as falling off exponentially with distance.[36] Recently, the more complex problem including both forward transfer and geminate recombination (BET) has also been solved exactly for the same model.[37−39] More recently, the exact treatment of photoinduced forward ET accompanied by geminate recombination has been extended to treat restricted geometries.[17a,19,20] This model considers one donor and N acceptors distributed on the surface of a spherical micelle, but the method has been claimed to be sufficiently general to be applicable to any spatial structure in a wide variety of restricted geometries.

Modeling of ET in a micellar system as that of transfer on a spherical surface is clearly a first approximation to the complicated spatial structure and dynamics of real micelles. This approximation may nevertheless be quite reasonable if the donor, acceptor and micellar system are carefully chosen.

In the present work, we have studied the dynamics of the photoinduced intermolecular ET reaction between perylene (Pe), which in its excited state acts as a donor, and the pyridinium moiety of the cetylpyridinium chloride (CPC) molecule, which itself forms a cationic micellar system in aqueous solution, as an acceptor. The dynamics of the ET process has been followed by monitoring the transient absorption of the excited state of the donor as well as the cation radical of Pe ($Pe^{\cdot+}$), formed as a result of ET, in real time with ultrafast time resolution (∼120 fs). The choice of this system is unique in many ways such that a simple ensemble-averaged theoretical model can be fruitfully adopted in explaining the dynamics of ET process in a micellar environment.[20] Previously, we reported the picosecond transient absorption study of ET reaction in Pe-CPC micellar system and established the efficient quenching of the excited singlet (S_1) state of Pe by CPC as well as very fast geminate recombination or BET process.[40] In that paper, we showed that CPC, below its critical micellar concentration (CMC), quenched the fluorescence of Pe at a diffusion-controlled rate. However, the quenching rate was observed to be extremely fast in the CPC micelle.

Selection of Pe as a donor has been made on the basis of the well-separated positions of the transient absorption bands of the S_1 state and that of $Pe^{\cdot+}$ in the visible region of the spectrum and the large extinction coefficient of absorption, as well as the long lifetime (∼5 ns) of the S_1 state of Pe in the absence of a quencher. In addition, Pe, being an aromatic hydrocarbon, is nearly insoluble in aqueous medium and resides exclusively in the micellar phase of the solution. Thus, it can reside either in the polar Stern layer (headgroup region) or in the nonpolar core region. Polarity of the headgroup region has been found to be nearly equal to that of ethanol ($\epsilon \approx 24$), in which Pe has good solubility.[34] It has been observed that aromatic probes prefer to be in the headgroup region of the cationic micelles.[34]

On the other hand, because the pyridinium moiety, which acts as the acceptor, is a part of the host micelle and the number of the quencher headgroup moiety in a CPC micelle is about 80,[34] an extremely fast quenching prevails. In addition, the position of the acceptor group, which resides on the surface of the micelle, is well-defined. Hence, it is an ideal model system to verify the validity of theoretical models treating the photoinduced ET and geminate recombination process on spherical micellar surfaces. This variety of intermolecular ET reactions, where one of the reactants is the self-reacting solvent bath itself, has previously been studied in a homogeneous medium.[41−43] In these studies, a reaction−diffusion prescription has been utilized to analyze the experimental results. However, the very description of diffusion is conceptually different in these treatments. In the present system, the close proximity of the donor and self-reacting micellar headgroups that act as acceptors and their large numbers in confined and isolated heterogeneous medium ensures ET in an ultrafast time scale. As a result, the choice of the ultrafast donor−acceptor ET system in the present study is equivalent to assuming that their movements are "frozen" within the time scale of ET such that the initial equilibrium distribution is maintained throughout the forward transfer event. Hence, the observed ET rates are determined by the effective distribution of pyridinium moieties of CPC around the excited Pe molecule. The present system, for the first time, has provided an opportunity to study the nondiffusive ET dynamics on the surface of a micelle, which we have realized with the help of ultrafast time-resolved measurements.

2. Experimental Section

Pe (Aldrich Chemical Co., U.S.A., 99.5% pure) was used as received. CPC (E. Merck, Germany), Triton X-100 (TX-100)

(Koch-Light, scintillation grade), Brij-35 (Pierce Chemical Co.), and sodium lauryl sulfate (SDS) (Fluka) were used as received. Triply distilled water was used for preparing the aqueous micellar solutions. At any micellar concentration that is higher than the CMC for a particular micellar system, the average micellar concentration can be defined as

$$[\mathrm{M}] = \frac{[\mathrm{S}] - \mathrm{CMC}}{N} \quad (1)$$

where [M] and [S] are the concentrations of the micelle and the surfactant, respectively, The value of CMC for CPC is 8.0×10^{-4} mol dm^{-3}, and N, the aggregation number of the micelle, is about 80 for CPC.[34] The concentration of the micelle was kept low enough so that it remained in monodispersed, spherical micellar phase.

Ground-state absorption and fluorescence spectra were recorded using an absorption spectrophotometer (Shimadzu, model UV160A) and a fluorescence spectrometer (Hitachi, model F4010), respectively. Fluorescence lifetimes were determined using a time-domain fluorescence spectrometer (Edinburgh Instruments, U.K., model 199), which used a hydrogen discharge flash lamp (fwhm $\approx$ 1 ns) for excitation of the sample and time-correlated single-photon counting (TCSPC) detection.

Relaxation processes in sub-500-ps time domain were measured using a femtosecond pump−probe transient absorption spectrometer, which used a laser system supplied by CDP-Avesta, Russia. The pulses of 50-fs duration and 6-nJ energy per pulse at 800 nm were obtained from a self-mode-locked Ti−sapphire laser oscillator, which was pumped by a 5-W diode-pumped solid-state laser. These pulses were amplified to generate 70-fs laser pulses of about 300-μJ energy at a repetition rate of 1 kHz using the chirped-pulse amplification (CPA) technique. The optical amplifier consisted of a pulse stretcher, a multipass amplifier pumped by an intracavity frequency-doubled Nd:YAG laser (6 W, 1 kHz), and a pulse compressor. Pump pulses at 400 nm were generated for excitation of the samples by frequency-doubling of one part of the 800-nm output of the amplifier in a 0.5-mm-thick β-barium borate (BBO) crystal, and the other part of the amplifier output was used to generate the white-light continuum (470−1000 nm) probe in a 2-mm-thick sapphire plate. The direction of polarization of the pump beam was fixed at the magic angle. Excitation energy was kept below 10 μJ/pulse, and the repetition rate of the pump beam was maintained at 500 Hz using a chopper. The sample solutions were kept flowing through a quartz cell of 1-mm path length. The decay dynamics at a particular wavelength region (10-nm width), which was selected using a pair of interference filters placed in front of the photodiodes to monitor the integrated intensity of the reference probe beam and the probe beam passing through the excited zone. The outputs of these photodiodes were routed through the boxcar integrators to an analog-to-digital converter (ADC) and computer for calculation of the optical density of the transient species at a particular delay time. The delay time between the pump and probe pulses was varied by using a stepper motor-driven single-axis linear motion stage (with 0.1-μm/step resolution), which was put on the path of the pump beam. The overall time resolution of the absorption spectrometer was determined to be about 120 fs by measuring the ultrafast growth of excited-state absorption (ESA) at different wavelengths in the 470−1000 nm region following the photoexcitation of tetraphenylprophyrin in benzene. These temporal profiles were also used to correct the effects of temporal dispersion on the time-resolved spectra through the adjustments of the positions of the zero delay between the pump and probe pulses at different wavelengths. The temporal profiles recorded using different probe wavelengths were fitted with up to three exponentially decaying or growing components by the iterative deconvolution method using a sech^2-type instrument response function with fwhm of 120 fs.

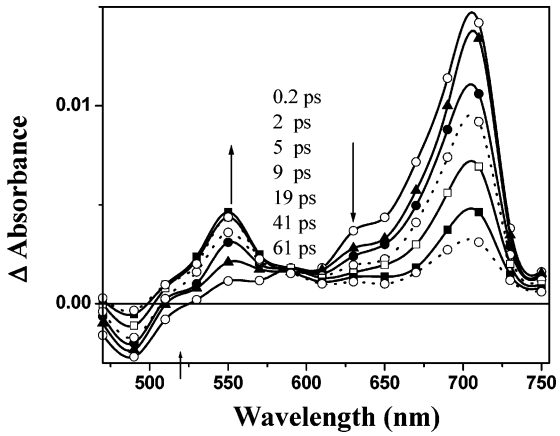

Figure 1. Time-resolved absorption spectra of the transients produced because of photoexcitation of perylene in the presence of 0.1 mol dm^{-3} of CPC in aqueous solution. The different delay times at which the spectra have been constructed are indicated.

3. Experimental Results

Figure 1 shows the time-resolved differential transient absorption spectra of Pe in the presence of 0.1 mol dm^{-3} CPC in aqueous solution following photoexcitation with 400-nm light of 70-fs duration. The spectrum recorded immediately after photoexcitation (i.e., at 0.2-ps delay time) has two important features. The ESA band in the 600−730 nm region with maximum at ca. 710 nm represents the $S_n \leftarrow S_1$ absorption of Pe.[44] The second feature is the negative absorption band in the 470−530 nm region with maximum at ca. 490 nm. Because the ground state of Pe in a micellar solution has little absorption in this wavelength region, but this wavelength region has good overlap with that of the fluorescence emission of Pe, the negative absorption band is assigned to the stimulated emission from the S_1 state of Pe due to amplification of the probe light. Both the ESA and the stimulated emission bands decay with increasing delay time, leading to concomitant development of another ESA band in the 510−590 nm region with maximum at ca. 550 nm. This corresponds to the absorption band of the $Pe^{\cdot+}$.[46] While the decay of both the ESA and the stimulated emission bands due to the S_1 state of Pe continues to occur up to 200 ps, the ESA band in the 510−575 nm region continues to grow up to about 45 ps to reach a maximum due to the formation of $Pe^{\cdot+}$ and then starts decaying at longer delay times (the time-resolved spectra corresponding to delay times longer than 60 ps have not been presented in Figure 1 to avoid congestion). The presence of a temporary isobestic point between the two ESA bands assigned to the S_1 state of perylene and $Pe^{\cdot+}$ provides clear evidence of the fact that, following photoexcitation of Pe, its S_1 state transfers an electron to the ground state of the CPC molecule to form $Pe^{\cdot+}$. Because both the hexadecyl group and Cl^- are not expected to quench the S_1 state of Pe, it is concluded that the observed quenching of the S_1 state of Pe is due to its interaction with the pyridinium group of the CPC molecule. The absorption maximum of the radical anion of CPC, $CPC^{\cdot-}$, which is formed because of this reaction, is reported to be at 280 nm, and this spectral region lies beyond the detection limit of our femtosecond transient absorption spectrometer.[46]

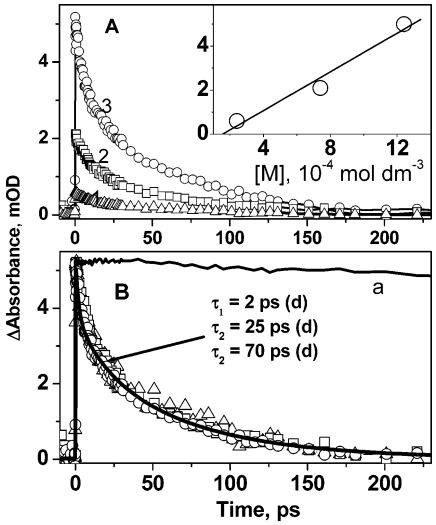

Figure 2. A. Temporal profiles for the decay of the S_1 state of perylene monitored at 710 nm following photoexcitation of perylene in the presence of 0.02 (1), 0.06 (2), and 0.1 (3) mol dm^{-3} of CPC in aqueous solutions. Inset: The plot of maximum absorbance of the temporal profiles 1, 2, and 3 vs the concentration of the micelle used. B. Three temporal profiles (1, 2, and 3), which have been shown in A, have been normalized to a value equal to the maximum absorbance of curve 3. The solid line represents the three exponential decay functions to best fit curve 3. The lifetimes are indicated. Curve a represents the temporal profile for the S_1 state of perylene monitored at 710 nm following photoexcitation of perylene in the presence of 0.1 mol dm^{-3} of TX-100 in aqueous solution.

Figure 2A presents the temporal profiles of the S_1 state of Pe monitored at 710 nm because of photoexcitation of Pe in aqueous CPC micellar solution with different concentrations of CPC (20, 60, and 100 mM). For each of these temporal curves, the transient absorption initially rises with the instrument response time (120 fs) and subsequently decays within 200 ps. We observe an increase of maximum absorbance, measured immediately after photoexcitation (e.g., at ~120-fs delay time), with an increase in the concentration of CPC. Pe can only reside inside the micelle because of its negligibly small solubility in water. Hence, an increase in the concentration of CPC results in an increase of the concentration of micelles and hence an increase in the solubility of Pe in the micellar phase. This argument is supported by the linear relationship between the maximum absorbance due to the S_1 state of Pe, which is measured immediately after photoexcitation, and the concentration of micelle in solution, which has been determined using eq 1 (inset of Figure 2A). This inference is also supported by the fact that the temporal profiles for the decay of the S_1 state of Pe are astonishingly identical in solutions with different concentrations of micelles (see Figure 2B, in which the maximum absorbance due to the S_1 state of Pe produced immediately after photoexcitation has been normalized to that of curve 3). These observations suggest that, in micellar solutions of CPC, dynamics of the S_1 state of Pe observed here is an intramicellar phenomenon. The temporal profiles presented in Figure 2B show that the decay of ESA due to the S_1 state of Pe is nonexponential, and they could be best fitted with a function consisting of three exponential decay terms having the decay lifetimes of 2, 25, and 70 ps. The temporal curves for the S_1 state of Pe in other micelles, such as TX-100 or Brij-35, which have no quencher moiety, have been recorded in the same time domain (i.e., sub-500 ps) and are also shown in Figure 2B (curve a). The fluorescence lifetimes of the S_1 state of Pe in TX-100 and Brij-35 micelles have been determined to be about 5 ns using the TCSPC technique.

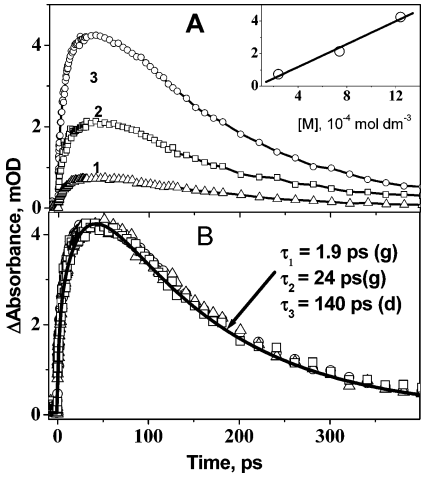

Figure 3. A. Temporal profiles for the evolution of perylene radical cation, $Pe^{\cdot+}$, monitored at 550 nm following photoexcitation of perylene in the presence of 0.02 (1), 0.06 (2), and 0.1 (3) mol dm^{-3} of CPC in aqueous solutions. Inset: The plot of maximum absorbance (corresponding to 45-ps delay time) on the temporal profiles 1, 2, and 3 vs the concentration of the micelle used. B. Three temporal profiles (1, 2, and 3), which have been shown in A, have been normalized to a value equal to the maximum absorbance of curve 3. The solid line represents the three exponential functions with two growing and one decay component to best fit curve 3. The lifetimes are indicated.

Figure 3A shows the temporal profiles monitored at 550 nm, which is the absorption maximum of $Pe^{\cdot+}$. They represent the dynamics of $Pe^{\cdot+}$ formed following the photoexcitation of Pe in micellar solutions with three different concentrations of CPC. Each of them show initial growth of $Pe^{\cdot+}$ up to about 45 ps, followed by its decay at longer delay time. Identical dynamics of $Pe^{\cdot+}$ in the presence of different concentrations of micelle (Figure 3B represents the three temporal curves 1, 2, and 3, each of which is normalized to the same maximum absorbance at 45 ps delay time), as well as the linear increase in the maximum absorbance of $Pe^{\cdot+}$ with an increase in the concentration of micelle (inset of Figure 3A), again support the intramicellar dynamics. Each of the temporal profiles (curves 1, 2, and 3), which represent the formation and subsequent decay of $Pe^{\cdot+}$, could be best fitted with a function having two exponentially growing components with lifetimes of 1.9 and 24 ps and one decay component with lifetime of 140 ps (Figure 3B). Two shorter-growth lifetimes (i.e., 1.9 and 24 ps), representing the process of formation of $Pe^{\cdot+}$, agree well with the two shorter decay lifetimes (2 and 25 ps) of the S_1 state of Pe. However, each of the temporal profiles, representing the evolution of $Pe^{\cdot+}$ in a time domain longer than 45 ps, is dominated by the decay of $Pe^{\cdot+}$ due to the geminate recombination process between $Pe^{\cdot+}$ and its sibling anion, $CPC^{\cdot-}$, and hence, the growth lifetime of the third component corresponding to the third component (lifetime of 70 ps) of the decay of the S_1 state of Pe could not be recovered from the fitting of the temporal profiles at 550 nm. However, a good agreement between the two growth lifetimes of $Pe^{\cdot+}$ with those of the major components of the S_1 state of Pe confirm the fact that $Pe^{\cdot+}$ is produced because of the interaction between the excited Pe molecule and CPC.

Now, it is important to establish that the ET interaction between Pe and CPC is the only process responsible for the nonexponential dynamics of the decay of the S_1 state of Pe. Because the ground state of CPC does not absorb beyond 300

nm, the energy level of the S_1 state of CPC is not expected to be lower than that of Pe, and hence, energy transfer from the S_1 state of Pe to CPC is not feasible. ET from the acceptor anion to a nearby neutral acceptor could not be considered, because there is no net driving force for this process and barriers to electron tunneling are generally large.[47]

The possibility of formation of $Pe^{\cdot+}$ through direct photoionization of Pe molecules has been investigated in TX-100 micelles under identical experimental conditions. TX-100 is not expected to quench the S_1 state of Pe. Curve a in Figure 2B represents the temporal profile of the transient absorbing at 710 nm on excitation of Pe with 400-nm light in TX-100 micelle. Temporal profiles recorded at other wavelengths in the 550−710 nm region have identical features. In addition, no absorption band characteristic of solvated electron has been observed in the 700−800 nm region in the time-resolved spectra of Pe in TX-100 micelles. All of these observations suggest that the possibility of formation of $Pe^{\cdot+}$ as a result of multiphoton ionization of Pe under the present experimental condition can be convincingly excluded.

Another possibility is that the nonexponential dynamics of the S_1 state of Pe may originate from the formation of excimer. Many aromatic molecules form excimers in the S_1 state due to interaction with another molecule in the ground state. Pe is also known to form an excimer, which is weakly emissive.[48] However, we have not obtained any evidence in favor of the formation of excimer from the fluorescence spectrum of Pe in TX-100. Although the fluorescence intensity of Pe is reduced substantially in CPC micelles, the shapes of the fluorescence spectra of Pe with different concentrations of CPC are similar to those observed in TX-100 and Brij-35 micelles with the concentration range of CPC used here for time-resolved measurements. In micellar solutions, the possibility of intermicellar excimer formation (i.e., an excited state located in one micelle diffusing out and meeting another molecule from a different micelle) is extremely low in the time scale of observation. However, the formation of excimer may result from intramicellar processes. This requires the presence of at least two Pe molecules in one micelle. In the present case, the maximum concentration of CPC surfactant used in the time-resolved experiments is 0.1 mol dm^{-3}, and the concentration of Pe solubilized in the micellar phase of this solution has been determined to be about 3×10^{-4} mol dm^{-3}. The micellar concentration is calculated to be 1.24×10^{-3} mol dm^{-3} in these solutions. This gives the mean occupancy factor (μ) per micelle of 0.24. According to the Poisson distribution function, the probability of finding n number of solute molecules in a micelle is given by

$$P(n) = \frac{\mu^n e^{-\mu}}{n!} \qquad (2)$$

assuming that the distribution of the solute in the micelle is random. Thus, we obtain $P(0) = 0.78$, $P(1) = 0.19$, $P(2) = 0.05$, and $P(3) = 0.013$. This indicates that the probability of intramicellar excimer formation is less than 5%. The possibility of contribution from the (Pe−Pe)* excimer in our transient absorption measurements in aqueous solution of the Pe-CPC system also can be excluded from the fact that the temporal profiles monitored at both 670 and 550 nm are independent of the concentration of CPC (see Figures 2 and 3).

The above arguments ensure that the quenching of the S_1 state of Pe is only due to ET interaction with the pyridinium moiety of the CPC molecule. These arguments also justify the fact that, in the absence of a driving force for the ET from the acceptor anion to a nearby neutral acceptor molecule, and because barriers for electron tunneling are generally large, the BET process takes place only between the $CPC^{\cdot-}$ and the original donor molecule residing in the same micelle.

SCHEME 1 : Schematic Representation of the Three-Level ET System[a]

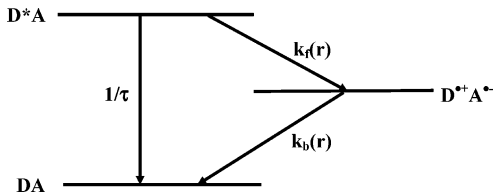

[a] Ground and excited states of the neutral donor−acceptor systems are designated as DA and D*A, respectively, and the donor cation−acceptor anion radical pair as $D^{\bullet+}A^{\bullet-}$. The rate processes, represented by $1/\tau$, $k_f(r)$, and $k_b(r)$, are the inverse fluorescence lifetime of the donor (in absence of the acceptor) and the forward and back ET processes, respectively.

Because Pe is nearly insoluble in water, the partitioning or exchange of Pe between the micelle and water is insignificant. However, the partitioning of Pe between the headgroup and the core regions is likely to occur in a very slow time scale. Fayer et al. showed that 2-ethylnaphthalene, which is water insoluble, exists preferentially in the headgroup region but is exchanged between the headgroup and the core region on a 5−10 ns time scale depending on the cationic micelle used.[49] Therefore, this exchange does not affect the dynamics of the ET reaction between Pe and CPC in micellar solution occurring in the sub-200-ps time domain.[49] Hence, the PET dynamics studied here is not influenced by diffusion that might arise from the dynamic partitioning of Pe between the headgroup and core regions of the micelle. Rather, it represents a true case of the distance-dependent ET process due to the spatial distribution of the acceptor molecules around the donor. Both the donor and acceptor molecules reside on the surface of the micelle. Recently, Swallen et al. also reported that the radial distribution function, $g(r)$, plays the dominant role in determining the observed ET dynamics.[13d] In the absence of diffusion, the observed ET rates will be determined by the effective distribution of the pyridinium moieties of CPC around the excited Pe molecules in the headgroup (surface) region of the micelle.

4. Theoretical Analysis

In this section, we will analyze the experimental observations in light of a theoretical approach for forward and reverse photoelectron transfer between the donor and the self-reacting headgroup moieties of the micelle, which serve as acceptors, on the surface of the micelle. In section 3 of this article, we have put forward several arguments to convince the reader that the present system can be modeled as "ET in a nondiffusive (solid solution-like) environment". The schematic of the bimolecular system and the respective energy diagram is presented in Scheme 1. Following photoexcitation of the donor−acceptor (DA) system by light pulse, the excited state of the donor molecule can be deactivated by radiative and nonradiative transitions to the ground state with the rate constant $1/\tau$. Alternatively, the excited donor−acceptor (D*A) system may follow another deactivation channel via forward ET from the excited neutral donor molecule to the acceptor molecule with the rate constant $k_f(r)$. This process of ET (forward transfer) creates the cationic radical of the donor ($D^{\cdot+}$) and the anionic radical of the acceptor ($A^{\cdot-}$), which we call the radical pair ($D^{\cdot+}A^{\cdot-}$). If energetically favorable, $A^{\cdot-}$ can transfer the electron

SCHEME 2 : Pictorial Illustration of the Pe-CPC Micelle System[a]

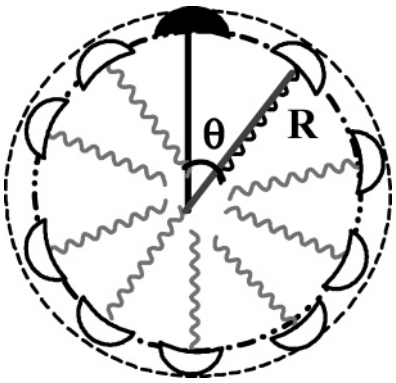

[a] The micelle is modeled as a hard sphere of radius *R*. The headgroup (or the Stern layer) of the micelle consists of the pyridinium moieties, which act as the electron acceptors and have been represented by the unfilled hard, curved disks. Each micelle contains only one Pe molecule as donor, represented by the solid filled disk, which also resides on the surface of the micelle. The distance between the donor and any particular acceptor moiety is the chord length, $r = R \sin \theta$.

back to $D^{\cdot+}$ with the rate constant $k_b(r)$ (BET is normally in the Marcus inverted regime).[6] Following the BET process, the system comes back to the ground electronic state. Note that we have been able to monitor the decay of the S_1 state of the excited state of Pe molecule and the subsequent growth of the $Pe^{\cdot+}$ from two different temporal curves monitored at two different wavelengths. Because both the decay of the S_1 state of Pe and the growth of $Pe^{\cdot+}$ follow multiexponential kinetics with the same time constants (see Figures 2B and 3A), we infer that there is a distribution of the ET rate constants, which arises because of the spatial distribution of the pyridinium moieties of the CPC molecules on the surface of the micelle around the Pe molecule. Thus, the use of distance-dependent forward and reverse rate constants is justified.

Recently, Fayer and co-workers presented a detailed theoretical analysis of the photoinduced forward ET and geminate recombination processes on the surface of a spherical micelle.[17b,20] Among a few assumptions made in this study, the most important one is that the concentration of the donor is kept very low such that no micelle contains more than one donor molecule, while the concentration of the acceptor is relatively higher so that one micelle contains a few acceptor molecules. In the case of the relatively higher concentration of the acceptors, the effects of the consideration of acceptor−acceptor-excluded volume become increasingly important. In the present study, the acceptors constitute the pure micellar headgroups, where the donor is selectively solvated. This implies that the donor is solvated in a sea of acceptors in a heterogeneous medium. In our case, the BET from $CPC^{\cdot-}$ occurs only to the original donor molecule, because each of the micelles contains only one donor and there is no net driving force for the ET process from the acceptor anion to the neutral acceptor, and barriers for electron tunneling are generally large; therefore, we will not consider any acceptor−acceptor ET. Moreover, because the experiments are carried out at a low concentration of the micelles, the intermicellar ET reaction has also not been considered.

In this model, the micelle is taken to be a hard sphere of radius *R*, which is equal to the difference between the true micellar radius (∼25 Å)[49] and the diameter (∼5.2 Å) of the pyridinium moiety, determined by using the atomic volume addition method of Edward (Scheme 2).[50] The donor (Pe) and acceptor (pyridinium) moieties exist as hard curved disks embedded in the surface region of the micellar sphere. The relevant ET distance is the chord distance, *r*, between the donor and acceptor. By taking the standard nonadiabatic mechanism of ET, we can determine its rate by the electron coupling matrix element (**V**) and by the Franck−Condon factor (*F*)-weighted density of states due to the molecular vibrations.

The dependence of the rate on the free energy gap, (ΔG), arises from the factor *F*, which, in turn, depends on the donor−acceptor spatial separation through the solvent reorganization energy. However, the distance dependence of the ET rate is mainly due to the factor **V**. Although the distance dependence of the solvent reorganization energy is prominent when the donor−acceptor separation is small, as in the present study, where the electron donor is embedded in an acceptor bath, we shall describe the distance dependence of ET through **V** only. This is purely an assumption which allows one to express the rates in the form of exchange interaction between molecules and independent of the Franck−Condon factor-weighted density of states and are given by

$$k_f(r) = \left(\frac{1}{\tau}\right) \exp\left[\frac{R_f - r}{a_f}\right] \tag{3}$$

$$k_b(r) = \left(\frac{1}{\tau}\right) \exp\left[\frac{R_b - r}{a_b}\right] \tag{4}$$

where $k_f(r)$ and $k_b(r)$ are the rate constants for the forward and back ET processes, respectively. τ^{-1} is the rate constant for relaxation of the excited state of the donor to the ground state in the absence of the ET process, and hence, τ is the lifetime of the excited state of the donor. R_f and R_b are the characteristic distance scales of the forward and reverse ET. The parameters a_f and a_b represent the falloff of the electronic wave function overlap between the neutral donor and acceptor (DA) and between the radical pair, ($D^{\cdot+}A^{\cdot-}$), respectively. We have ignored the distance dependence of the rates that enters through the Franck−Condon factor for two reasons. First, for the forward transfer event, the rate would have depended on too many parameters. As a result, any analysis of the experimental data would have required a large number of input parameters, many of which were unknown, and thus, this would have involved too much free-parameter dependence for any meaningful application of a given model. Second, for the reverse transfer, which normally occurs in the inverted region, it would have required knowledge of the high-frequency vibrational modes, and thus, a quantum mechanical treatment was inevitable. This again would have required too many input parameters. Thus, we chose a simpler form for the rates[20] given by eqs 3 and 4, which will simplify the analysis of the experimental data in light of the model presented here and helps one to understand the basic features of the transfer events in a self-reactive restrictive environment.

Now, we shall turn to the theoretical calculation of the temporal profiles of the S_1 state of Pe (to obtain the forward transfer rate) and $Pe^{\cdot+}$ (to obtain the BET rate). They are given in terms of the probability of survival of the excited state, $P_{ex}(t)$ and that of the radical cation, $P_{ct}(t)$. The latter contains the contributions from both the formation and decay kinetics of the cation radical. To obtain $P_{ex}(t)$, one has to calculate an ensemble average over spatial distribution of the reacting system. Let us start with one donor and one acceptor. After direct

excitation of the donor, the probability that the donor is still excited at time t is given by

$$P_{ex}(r, t) = \exp[-k_f(r)t] \tag{5}$$

In eq 5, the term due to the natural decay of the donor, $\exp(-t/\tau)$, is not included for simplifying the calculation. However, the same can be included in the final expression (see below). Because our interest is in the average over all possible configurations of the system, the decay profile of the donor is given by

$$P_{ex}(t) = \langle P_{ex}(r, t)\rangle = \sum P(r) \exp[-k_f(r)t] \tag{6}$$

where the sum is taken over all possible configurations and $P(r)$ is the probability of occurrence of a given configuration. In the continuum limit, $\sum P(r) \rightarrow \int_0^\infty p(r) r^{\Delta-1}\, dr$, where Δ is the dimensionality of the system and $p(r)$ is the equilibrium distribution of the acceptor with respect to the donor. Hence, eq 6 can be written in the form

$$P_{ex}(t) = \int_0^\infty p(r) \exp[-k_f(r)t] r^{\Delta-1}\, dr \tag{7}$$

eq 7 describes the configurationally averaged decay profile of the donor when there is one acceptor in the system. However, the present system consists of 1 donor (Pe molecule) and N acceptors (which are 80 CPC molecules) residing on the surface of a spherical micelle. The experimental observable is the statistical average over all possible arrangements of the N acceptors. Hence, with $p(\mathbf{r}_1, \mathbf{r}_2, \cdots, \mathbf{r}_N)$ denoting the probability density of finding the acceptor molecule 1 at a position $\mathbf{r}_1$, 2 at $\mathbf{r}_2$, and so on, eq 7 needs to be modified to represent the many-particle observable. Because the positions of the acceptors are uncorrelated and interactions between the donor−acceptor pairs are independent of each other, the joint probability density function can be factored into a two-particle density function (i.e., $p(\mathbf{r}_1, \mathbf{r}_2, \cdots, \mathbf{r}_N) = p(r)^N$. With this modification, for a many-particle system, eq 7 is modified to eq 8[51]

$$P_{ex}(t) = \{\int_0^\infty p(r) \exp[-k_f(r)t] r^{\Delta-1}\, dr\}^N \tag{8}$$

Finally, because natural decay of the donor and ET are two independent parallel processes, the ensemble-averaged excitation decay of the donor is given by

$$P_{ex}(t) = \exp(-t/\tau)\{\int_0^\infty p(r) \exp[-k_f(r)t] r^{\Delta-1}\, dr\}^N \tag{9}$$

For the point particles distributed on the surface of a micelle and when the distance is calculated from a donor situated at the north pole of the spherical surface (Scheme 2), the equilibrium distribution function of the acceptors is given by[20]

$$p(r) r^{\Delta-1}\, dr = (r/2R^2)\, dr \tag{10}$$

Allowing for the finite dimensionality of the system, we can modify eq 9 to

$$P_{ex}(t) = \exp(-t/\tau)\left\{\frac{1}{2R^2}\int_0^{2R} \exp[-k_f(r)t] r\, dr\right\}^N \tag{11}$$

Any realistic particles, however, have finite sizes. This limits the distance of closest approach between the particles. On the other hand, the rates expressed in the form of exchange interaction (cf., eqs 3 and 4) have significantly higher values at shorter intermolecular distances. Thus, a consideration of the donor−acceptor excluded-volume effect, which excludes ET happening at shorter distances, is absolutely necessary in order to analyze the experimental data. To include the effect of donor−acceptor excluded volume, one needs to change the lower limit of the above integration to the distance of closest approach, r_m, between the donor and an acceptor. Along with this, after a due consideration of the normalization constant, eq 11 changes to[20]

$$P_{ex}(t) = \exp(-t/\tau)\left\{\frac{2}{4R^2 - r_m^2}\int_0^{2R} \exp[-k_f(r)t] r\, dr\right\}^N \tag{12}$$

Note that, in this expression, except for the consideration of the distance of closest approach, the point−particle assumption and the separability of the joint probability distribution function is still assumed to hold good.

Calculation of the temporal profile of the donor cation is more involved, because it depends on the details of the forward transfer. The ensemble averaging to move over to many-particle description is evidently not straightforward.[20] If acceptor 1 is at position r_1, 2 at r_2, ..., N at r_N (denoted as $\bar{r}$), with the ith acceptor anion positioned at r_i, then the probability of survival of the donor cation before it is geminately recombined is given as

$$\frac{\partial P_{ct}^i(\bar{r}, t)}{\partial t} = k_f(r_i) P_{ex}(\bar{r}, t) - k_b(r_i) P_{ct}^i(\bar{r}, t) \tag{13}$$

Solution of this equation is given by

$$P_{ct}^i(r, t) = \frac{k_f(r_i)}{\left(\frac{1}{\tau}\right) - k_b(r_i) + \sum_{j=1}^N k_f(r_j)}\left\{\exp[-k_b(r_i)t] - \exp\left(-\frac{t}{\tau}\right)\exp[-\sum_{j=1}^N k_f(r_j)t]\right\} \tag{14}$$

The ensemble average of this equation has been performed exactly using the procedure of Lin et al.,[52] and the following expression for the ensemble average of $P_{ct}(t)$ has been obtained.[20]

$$P_{ct}(t) = \frac{2N}{4R^2 - r_m^2}\int_{r_m}^{2R}\int_{t'=0}^{t} k_f(r) \exp\left(\frac{-t'}{\tau}\right) \exp[-k_f(r)t'] \exp[-k_b(r)(t - t')] \times \left\{\left(\frac{2}{4R^2 - r_m^2}\right)\int_{r'=r_m}^{2R} \exp[-t' k_f(r')] r'\, dr'\right\}^{N-1} dt' r\, dr \tag{15}$$

This kind of lengthy expression is quite inevitable for a reversible reaction, such as the present one, and can be thought of as a convolution integral, where the reverse reaction can be seen to be "convoluted" by the forward transfer event. The above equation can also be obtained from a simple argument that follows from the fact that the probability, Z, that an electron is transferred from an excited donor to an acceptor located between r and $r + dr$ at time t is given by

$$Z = \frac{2N}{4R^2 - r_m^2} k_f(r) \exp\left(\frac{-t}{\tau}\right) \exp[-k_f(r)t]\left\{\left(\frac{2}{4R^2 - r_m^2}\right)\int_{r'=r_m}^{2R} \exp[-t k_f(r')] r'\, dr'\right\}^{N-1} \tag{16}$$

Following the forward transfer, the acceptor anions are produced between r and $r + dr$ at time t, which then undergo reverse reaction with a rate constant of $k_b(r)$. Clearly then, the probability of finding the donor cations (or the acceptor anions) in a reactive state is the convolution of eq 16 over time and space as given by eq 15.

Both of the expressions (eqs 12 and 15) represent the experimental observable and reveal the full distance dependence of the ET reaction with due allowance for the donor−acceptor excluded volume. Clearly, acceptor−acceptor excluded volume[17b,20] also affects the transfer kinetics especially at a high acceptor concentration, such as in the present experimental system. However, the calculation of the number of surfactant molecules ($N = 80$) at the CMC of CPC does take into account the molecular size of the pyridinium moiety that is distributed over the surface of the micelle and acts as an acceptor. As a result, the very facts that the reaction takes place in a heterogeneous medium and that the donor is solvated in a pure microenvironment of 80 acceptors fortuitously take into account the acceptor−acceptor excluded volume. As a result, eqs 12 and 15 can as such be used to analyze the experimental results and can be thought of as including the acceptor−acceptor excluded-volume effect through the specific number of acceptors, which has been attained with the due consideration of acceptor molecular size. Equations 12 and 15 have no analytical solutions, and the integrals have been evaluated through numerical methods.

Equations 12 and 15 hold well for the kinetics of the reactions in a nondiffusive environment, which we intend to apply in liquid solution, where one can naively expect that the diffusion is prominent. However, we have discussed earlier that our choice of the donor−acceptor system in the self-reactive surface of a micellar system renders the kinetics to be too fast to consider any material diffusion in the time scales of ET and BET reactions. In other words, the donor confined and submerged in pure-acceptor environment efficiently leads to the completion of the reaction before the diffusive phenomenon sets in. Thus in the time scale of the ET reaction, although the reaction is taking place in a liquid solution, the molecular motion has been assumed to be frozen and the reacting system can be thought of as a rigid solid solution. To further substantiate this claim, we have also calculated the distribution of ET distances (see below).

Distribution of ET distances, $Y(r)$, is defined in such a way that $Y(r)\,dr$ represents the probability of ET over a distance between r and $r + dr$. Note that the distribution of ET distances cannot be fully described by the distance-dependent first-order rate constant alone[53] (cf., eq 3). To properly take into account the distribution of ET distances, one has to necessarily consider the first-order rate constant along with the second-order survival probability of the reactant, $P_{ex}(t)$. Theory for $Y(r)$ has been previously developed,[53] and the success and utility of the concept has been verified.[54] Following the definition of the probability that an excited donor transfers an electron to a donor located between r and $r + dr$ (cf., eq 16), distribution of ET distances on the surface of the micelle as a function of time, $Y(r, t)$, is found to be given by

$$Y(r, t) = \int_0^t Z\,dt \qquad (17)$$

where Z is given by eq 16. Solution of eq 16 for a system consisting of one donor and N acceptors can be put into eq 17, and $Y(r, t)$ can be obtained by numerical integration.

Figure 4A,B shows the theoretically calculated values of $P_{ex}(t)$ and $P_{ct}(t)$ representing the temporal profiles of the forward and reverse ET, respectively, for the Pe-CPC system in a micellar solution of CPC and compared with the experimentally determined temporal curves representing the decay of the S_1 state of Pe and the temporal evolution of the $Pe^{\cdot+}$, monitored at 710 and 550 nm, respectively. For these calculations, we used the following parameters: $R = 19.8$ Å, $N = 80$, $\tau = 5$ ns, $R_f = 12.2$ Å, $R_b = 12.2$ Å, $a_f = a_b = 1$ Å. The distance of closest approach (r_m) is taken to be 6.4 Å, which is the sum of the van der Waals radii of the Pe molecule and the pyridinium moiety, determined by the volume addition method prescribed by Edward.[50] The values of the ET parameters are obtained from the best fitted results of the temporal profiles for the S_1 state of Pe and that of the radical cation $Pe^{\cdot+}$. While analyzing the experimental data of the excited-state decay profile of Pe using eq 12, we have normalized the experimental decay profile to unity at zero time. Similarly, in Figure 4B, the results obtained from eq 15 has been scaled to match with the maximum absorption of $Pe^{\cdot+}$. The curves are plotted on both the linear and logarithmic time scales for an illustrative purpose to show the full time dependence of the process. In the logarithmic plot, the curve is nearly flat at very short time because of the donor−acceptor excluded volume, and the shape of the $P_{ex}(t)$ curve suggests that the ET dynamics span over a wide range of the time scale reflecting the spatial distribution of the acceptors with respect to the donor on the micellar surface. It is indeed gratifying to note that the forward ET parameters extracted from fitting with the experimental results in Figure 4A that serve as an input while analyzing the temporal profile of $Pe^{\cdot+}$ in Figure 4B could satisfactorily reproduce the experimental profile in the entire time range.

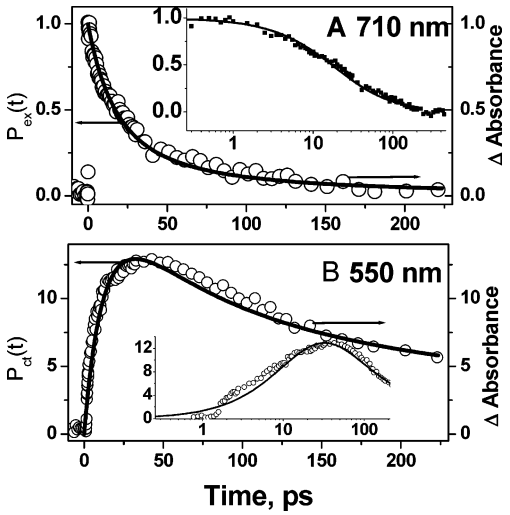

Figure 4. A. Decay profile of the excited state of Pe monitored at 710 nm (open symbols), and the line shows the theoretically calculated value of $P_{ex}(t)$. The experimental decay of the donor absorption (cf. Figure 2B) has been normalized to unity. ET parameters used while calculating the decay trace theoretically are $R = 19.8$ Å, $N = 80$, $\tau = 5$ ns, $R_f = 12.2$ Å, $a_f = 1$ Å. Inset shows the comparison in logarithmic time scale. B. Geminate recombination profile of $Pe^{\cdot+}$ monitored at 550 nm shown by open symbols. The line shows the theoretical results obtained from the calculation of $P_{ct}(t)$. In comparison with experiment, the theoretical $P_{ct}(t)$ values are scaled to the maximum of the experimental geminate profile. The parameters used to obtain the theoretical results are $R = 19.8$ Å, $N = 80$, $\tau = 5$ ns, $R_f = 12.2$ Å, $R_b = 12.2$ Å, $a_f = a_b = 1$ Å. Inset shows the comparison in logarithmic time scale.

In Figure 5, we have presented the distribution of ET distances at various time after the initiation of the reaction. The figure clearly depicts that the ET is long-range in nature and distance dependent. The curves in this figure, the shape of which does

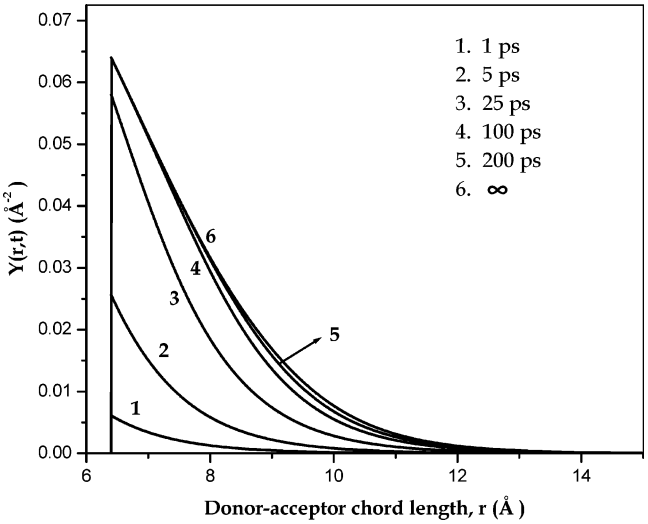

Figure 5. Distribution of electron-transfer distances on the surface of the micellar system in a nondiffusive environment plotted as a function of donor−acceptor chord length *r*. Curves represent the progress of the reaction at various times after excitation. ET parameters used are the same as in Figure 4A.

not change with time, depict the increased participation of acceptors as a function of time at any given distance away from the north pole of the micellar surface where the donor is assumed to be fixed. A closer look at this figure reveals that at any given time the probability of electron transfer is maximum in and around the contact distance. However in solid solutions,[53] as the present ultrafast experimental system is treated to be, at short times the excited donors undergo ET reaction with the closely held fewer acceptors. At long times, the surviving donors have the possibility to transfer electrons to a larger number of acceptors located only at long distances. Therefore, the distribution of ET in solid solutions should grow initially at shorter distances and then fall of at long distances as the excited donors are consumed. As a result, the distribution of ET in solid solutions is expected to give rise to a bell-shaped curve when plotted as a function of distance away from the space-fixed donor. Clearly, the curves plotted in Figure 5 do not conform to this expectation. The reasons behind this can be manifold: for example, the spatial range of the first-order rate constant (cf., eq 3); a relatively longer-range first-order ET rate is more likely to give rise to a bell-shaped $Y(r, t)$ curve than a shorter-range one. The concentration of the acceptors could also be a factor deciding the shape of the $Y(r, t)$ profiles. In the present case of the ET system, in the microheterogeneous medium the donor is confined to a small-volume element and embedded in a sea of self-reactive micellar headgroups that serve as acceptors ($N = 80$). This essentially gives rise to a sufficiently high local concentration of acceptors in the immediate neighborhood of the excited donor such that the donor excitation gets quenched through ET to closely held acceptors, and the reaction kinetics is dominated by this variety of acceptors. Thus, the high local concentrations of acceptors eventually rules out the possibility of occurrence of ET to relatively long-distant acceptors (which can give rise to bell-shaped $Y(r, t)$ profile). And, as a consequence of this, the shape of the $Y(r, t)$ profiles as presented in Figure 5 at any given time show a monotonic behavior (as a function of r), a signature of distance-dependent ET.

As stated above, because the concentration of quenchers is high, the profiles for the distribution of ET distances saturates within 200 ps, which is a reflection of the fact that the reaction completes within this ultrafast time scale. During this time, the farthest distance up to which the reaction proceeds is ∼15 Å. Assuming a diffusion coefficient, D, of ∼5 Å^2/ns, normally encountered in micellar surfaces,[17c,18] the time that would have been taken by the acceptors to diffuse from this farthest distance is 45 ns. Whereas to diffuse a distance equivalent to the contact distance, r_m, the necessary time (r_m^2/D) required is 8 ns. Contrary to this, the experimentally observed ET time (∼200 ps) is much shorter than either of these time scales. Thus, the basic assumption that the transfer occurs before the diffusive interplay starts influencing the kinetics is justified and convincing, which has been the main theme of the present theoretical analysis.

5. Conclusions

Intermolecular ET dynamics from the excited singlet state of Pe to the pyridinium moiety of the CPC micellar system has been investigated by monitoring both the decay of the S_1 state of Pe and the formation and decay of $Pe^{\cdot+}$ in real time using the femtosecond transient absorption spectroscopic technique with 120-fs time resolution. Following optical excitation, Pe undergoes ultrafast ET to the pure acceptor pool, which happens to be the headgroup of the host micellar system. $Pe^{\cdot+}$ thus formed immediately undergoes geminate recombination. Neat and careful experiments are designed and performed to support the conclusion that intramicellar ET from Pe to CPC is the sole mechanism behind the quenching of the excited state of Pe. It has been observed that the ET is complete within ∼200 ps.

A statistical mechanical theory for the donor−acceptor system distributed on the surface of the micelle has been employed to analyze the experimental data. We have provided enough evidence to convincingly prove that the transfer can be described by nondiffusive dynamics. While employing the theory, we have given due consideration to the donor−acceptor excluded volume. Because the number of pyridinium (acceptor) moieties ($N = 80$) is attained with due allowance for the molecular size, our choice of the reacting system fortuitously excludes the requirement of any separate consideration of acceptor−acceptor excluded-volume effect, which gains importance when the acceptor concentration is high. Thus, the possibility of overestimation of the number of spatial configurations could be avoided. The ET parameters extracted from the decay of the excited Pe could be successfully used while analyzing the geminate recombination profile. We have also emphasized that the distance-dependent ET cannot be solely predicted with the help of a first-order rate constant. Rather, a systematic approach toward this leads to the concept of distribution of ET distances, $Y(r, t)$, as given by eq 14. By calculating $Y(r, t)$, we have been able to describe the spatiotemporal progress of the reaction in a nondiffusive self-reactive restricted environment.

Acknowledgment. Authors gratefully acknowledge one of the anonymous reviewers of the manuscript for creative and constructive suggestions concerning the formulation of distribution of the electron transfer distances concept. Authors are also thankful to Dr. T. Mukherjee, Associate Director, Chemistry Group, BARC, Mumbai, for his constant encouragement.

References and Notes

(1) *Photoinduced Electron Transfer, Parts A − D*; Fox, M. A., Chanon, M., Eds.; Elsevier: New York, 1988.

(2) *Electron Transfer From Isolated Molecules to Biomolecules*; Jortner, J., Bixon, M., Eds.; J. Wiley: New York, 1999; Vols. 106−107.

(3) *Electron Transfer in Inorganic, Organic and Biological Systems*; Bolton, J. R., Mataga, N., Mclendon, G. L., Eds.; The American Chemical Society: Washington, DC, 1991.

(4) Special issue on Electron Transfer. *Chem. Rev.* **1992**, *92*.

(5) Rochester Symposium on Charge Transfer in Restricted Geometries. *J. Phys. Chem.* **1991**, *96*, 2777.

(6) Marcus, R. A.; Sutin, N. *Biochim. Biophys. Acta* **1985**, *811*, 265.

(7) *Advances in Photosynthesis and Respiration*; Govindjee, Ed.: Kluwer Academic: Amsterdam, 1995−2004; Vols. 1−15.

(8) Pelizetti, M.; Schiavello, M. *Photochemical Conversion and Storage of Solar Energy*; Kluwer: Dordrecht, 1997.

(9) O'Regan, B.; Gratzel, M. *Nature* **2001**, *353*, 737.

(10) Aviram, A., Ratner, M. M., Eds.; *Molecular Electronics: Science and Technology*; New York Academy of Sciences: New York, 1998; Vol. 852.

(11) (a) Carter, F. L., Ed.; *Molecular Electronic Devices*; Dekker: New York, 1982; Vol. I. (b) Carter, F. L., Ed.; *Molecular Electronic Devices*; Dekker: New York, 1987; Vol. II.

(12) Skourties, S. S.; Beratan, D. N. Theories of Structure−Function Relationships for Bridge-Mediated Electron-Transfer Reactions. In *Electron Transfer − From Isolated Molecules to Biomolecules*; Jortner, J.; Boxon, M., Eds.; Advances in Chemical Physics Series; John Wiley: New York, 1999; Vol. 106, Part 1, p 377.

(13) (a) Tavernier, H. L.; Kalashnikov, M. M.; Fayer, M. D. *J. Chem. Phys*. **2000**, *113*, 10191. (b) Tavernier, H. L.; Fayer, M. D. *J. Chem. Phys*. **2001**, *114*, 4552. (c) Weidemaier, K.; Tavernier, H. L.; Swallen, S. F.; Fayer, M. D. *J. Phys. Chem. A* **1997**, *101*, 1889. (d) Swallen, S. F.; Weidemaier, K.; Fayer, M. D. *J. Chem. Phys*. **1996**, *104*, 2976.

(14) (a) Iwai, S.; Murata, S.; Tachiya, M. *J. Chem. Phys*. **1998**, *109*, 5963. (b) Burcel, L.; Mostafavi, M.; Tachiya, M. *J. Phys. Chem. A* **1999**, *103*, 5882.

(15) Yoshihara, K.; Tominaga, K.; Nagasawa, Y. *Bull. Chem. Soc. Jpn.* **1995**, *68*, 696.

(16) Roy, S., Bagchi, B. *J. Chem. Phys.* **1994**, *100*, 8802.

(17) (a) Tavernier, H. L.; Barzykin, A. V.; Tachiya, M.; Fayer, M. D. *J. Phys. Chem. B* **1998**, *102*, 6078. (b) Swallen, S. F.; Weidemaier, K.; Fayer, M. D. *J. Phys. Chem.* **1995**, *99*, 1856. (c) Weidemaier, K.; Tavernier, H. L.; Swallen, S. F.; Fayer, M. D. *J. Phys. Chem. B* **1997**, *101*, 9352.

(18) Sano, H.; Tachiya, M. *J. Chem. Phys.* **1981**, *75*, 2870.

(19) Tavernier, H. L.; Laine, F.; Fayer, M. D. *J. Phys. Chem. A* **2001**, *105*, 8944.

(20) Weidemaier, K.; Fayer, M. D. *J. Chem. Phys.* **1995**, *102*, 3820.

(21) Kumbhakar, M.; Nath, S.; Pal, H.; Sapre, A. V.; Mukherjee, T. *J. Chem. Phys.* **2003**, *119*, 388.

(22) Pal, S. K.; Mondal, D.; Sukul, D.; Bhattacharyya, K. B. *Chem. Phys.* **1999**, *249*, 63.

(23) Hammarström, L.; Norrby, T.; Stenhagen, G.; Martensson, J.; Akemark, B.; Almgren, M. *J. Phys. Chem. B* **1997**, *101*, 7494.

(24) Gray, H. B.; Winkler, J. R. *Annu. Rev. Biochem.* **1996**, *65*, 537.

(25) (a) Lewis, F. D.; Wu, T.; Zhang, Y.; Letsinger, R. L.; Greenfield, S. R.; Wasielewski, M. R. *Science* **1997**, *277*, 673. (b) Lewis, F. D.; Kalgutkar, R. S.; Wu, Y. S.; Liu, X. Y.; Liu, J. Q.; Hayes, R. T.; Miller, S. E.; Letsinger, R. L.; Greenfield, S. R.; Wasielewski, M. R. *J. Am. Chem. Soc.* **2000**, *122*, 12346.

(26) Tavernier, H. L.; Fayer, M. D. *J. Phys. Chem. B* **2000**, *104*, 11541.

(27) Arkin, M. R.; Stemp, E. D. A.; Turro, C.; Turro, N. J.; Burton, J. K. *J. Am. Chem. Soc.* **1996**, *118*, 2267.

(28) Liu, Y. P.; Newton, M. D. *J. Phys. Chem.* **1994**, *98*, 7612.

(29) Lewis, F. D., Liu, J., Weigel, W., Rettig, W., Kurnikov, I. V., Beratan, D. N. *Proc. Natl. Acad. Sci. U.S.A.* **2002**, *99*, 12536. Gray, H. B.; Winkler, J. R. In *Electron transfer in Chemistry*; Balzani, V., Ed.; Wiley: Weinheim, Germany, 2001; Vol. 3, pp 3−23. Clery, D. *Science* **1995**, *267*, 1270.

(30) Okada, A.; Bandyopadhyay, T.; Tachiya, M. *J. Chem. Phys*. **1999**, *110*, 3509. Okada, A.; Bandyopadhyay, T. *J. Chem. Phys.* **1999**, *111*, 1137.

(31) (a) Aota, H.; Araki, S.; Morishima, Y.; Kamachi, M. *Macromolecules* **1997**, *30*, 4090. (b) Morishima, Y.; Aota, H.; Saegusa, K.; Kamachi, M. *Macromolecules* **1996**, *29*, 6505.

(32) Fox, M. A. Photoinduced Electron Transfer in Arranged Media. In *Topics in Current Chemistry*; Mattay, J., Ed.: Springer-Verlag: Berlin, 1991; Vol. 159, p 67.

(33) Sutin, N. Nuclear and Electronic factors in Electron Transfer: Distance dependence of Electron Tarnsfer Rates. In *Electron transfer in inorganic, organic and biological systems*; Bolton, J. R., Mataga, N., Mclendon, G. L., Eds.; The American Chemical Society: Washington, DC, 1991; p 25.

(34) Kalyanasundaram, K. *Photochemistry in Microheterogeneous Systems*; Academic Press: New York, 1987.

(35) Wasielewiski, M. R. Distance Dependencies of Electron Transfer Reactions. In *Photoinduced Electron Transfer, Part A: Conceptual Basis*; Fox, M. A., Chanon, M., Eds.; Elsevier: New York, 1988, p 161.

(36) Tachiya, M.; Mozumder, A. *Chem. Phys. Lett.* **1974**, *28*, 87.

(37) Fayer, M. D.; Song, L.; Swallen, S. F.; Dirfman, R. C.; Weildemaier, K. In *Ultrafast Dynamics of Chemical System*; Simon, J. D., Ed.; Kluwer Academic: Amsterdam, 1994; p 37.

(38) Lin, Y.; Dorfman, R. C.; Fayer, M. D. *J. Chem. Phys.* **1989**, *90*, 159.

(39) Dorfman, R. C.; Tachiya, M.; Fayer, M. D. *Chem. Phys. Lett.* **1991**, *179*, 152.

(40) Palit, D. K.; Sapre, A. V.; Mittal, J. P. *Chem. Phys. Lett.* **1997**, *269*, 286.

(41) Shirota, H.; Pal, H.; Tominaga, K.; Yoshihara, K. *J. Phys. Chem. A* **1998**, *102*, 3089.

(42) Saik, V. O.; Goun, A. A.; Fayer, M. D. *J. Chem. Phys.* **2004**, *120*, 9601.

(43) Iwai, S.; Murata, S.; Kato, R.; Tachiya, M.; Kikuchi, K.; Takahashi, Y. *J. Chem. Phys*. **2000**, *112*, 7111.

(44) Kawai, K.; Yamamoto, N.; Tsubomura, H. *Bull. Chem. Soc. Jpn.* **1970**, *43*, 2266.

(45) Shida, T. *Electronic Absorption Spectra of Radical Ions*; Elsevier Science Publisher: Amesterdam, 1988.

(46) Szajdzinska-Pietek, E.; Gebiski, J. L.; Kroh, J. *Radiat. Phys. Chem*. **1992**, *39*, 117.

(47) Devault, D. Q. *Rev. Biophys.* **1980**, *13*, 387.

(48) Birks, J. B. *Photophysics of Aromatic Molecules*; Wiley-Interscience: London, 1970.

(49) Van der Auweraer, M.; Roelants, E.; Verbeeck, A.; De Schryver, F. C. In *Surfactants in Solutions*; Mittal, K. L., Ed.; Plenum Publishing Corporation: New York, 1989; Vol. 7.

(50) Edward, J. T. *J. Chem. Educ*. **1970**, *46*, 373.

(51) Tachiya, M. *Radiat. Phys. Chem*. **1983**, *21*, 167.

(52) Lin, Z.; Cai, J. J.; Scriven, L. E.; Davis, H. T. *J. Phys. Chem*. **1994**, *98*, 5984.

(53) Murata, S.; Tachiya, M. *J. Phys. Chem*. **1996**, *100*, 4064.

(54) Bandyopadhyay, T.; Seki, K.; Tachiya, M. *J. Chem. Phys*. **2000**, *112*, 2849.